

Supplementary Materials: Non-Covalent Interactions in Hydrogen Storage Materials $\text{LiN}(\text{CH}_3)_2\text{BH}_3$ and $\text{KN}(\text{CH}_3)_2\text{BH}_3$

Filip Sagan, Radosław Filas and Mariusz P. Mitoraj

Table S1. Overall bonding energies ΔE_{total} (in kcal/mol) describing the interaction between two dimeric fragments in $\text{LiN}(\text{CH}_3)_2\text{BH}_3$ (the fragmentation as shown in Figure 2A) from Gaussian program.

Gaussian	BLYP-D3	MP2/6-311 + G **	PBE-D3/6-311 + G **	MO6-2X/6-311 + G **	WB97xd/6-311 + G **
ΔE_{total}	-29.57	-29.19	-29.00	-27.72	-31.20

Table S2. ETS energy decomposition results describing the interaction between two dimeric fragments in $\text{LiN}(\text{CH}_3)_2\text{BH}_3$ (the fragmentation as shown in Figure 2A) from ADF program.

ADF	BLYP-D3/TZP	PBE-D3/TZP	BP86-D3/TZP
ΔE_{total}	-29.67	-29.44	-29.95
ΔE_{orb}	-18.17	-17.79	-18.31
ΔE_{elstat}	-35.56	-34.16	-35.48
ΔE_{Pauli}	29.48	27.78	30.21
ΔE_{disp}	-11.38	-11.03	-11.75
ΔE_{dist}	6.06	6.00	5.10

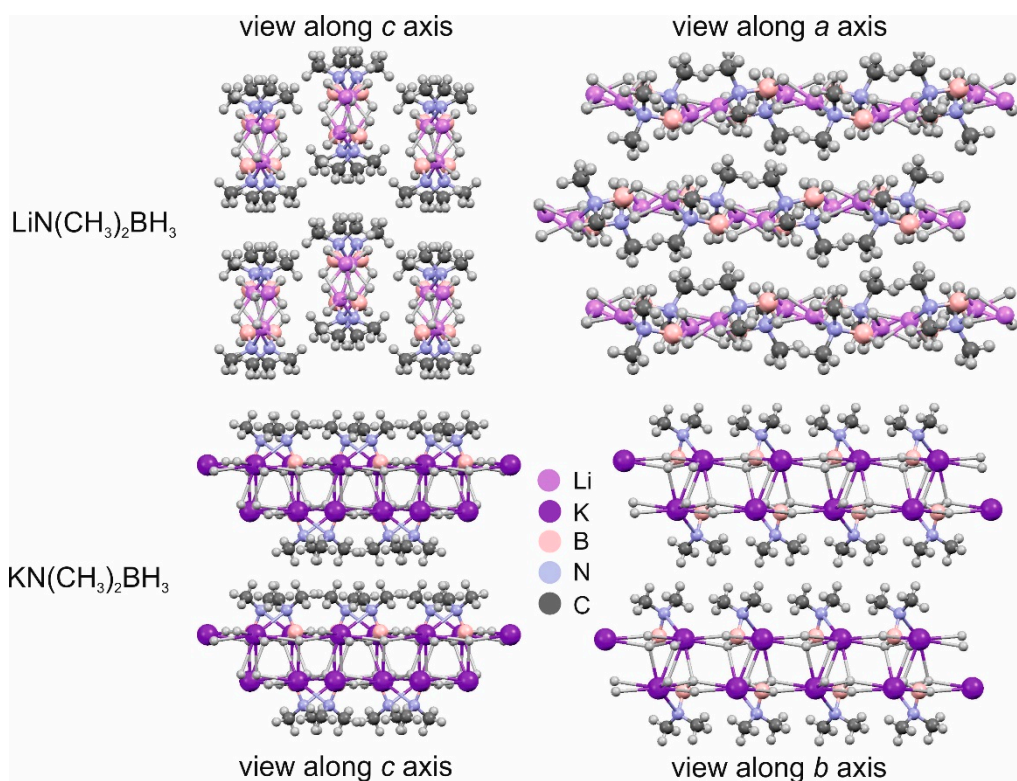


Figure S1. Alternative views of $\text{LiN}(\text{CH}_3)_2\text{BH}_3$ and $\text{KN}(\text{CH}_3)_2\text{BH}_3$ crystals.

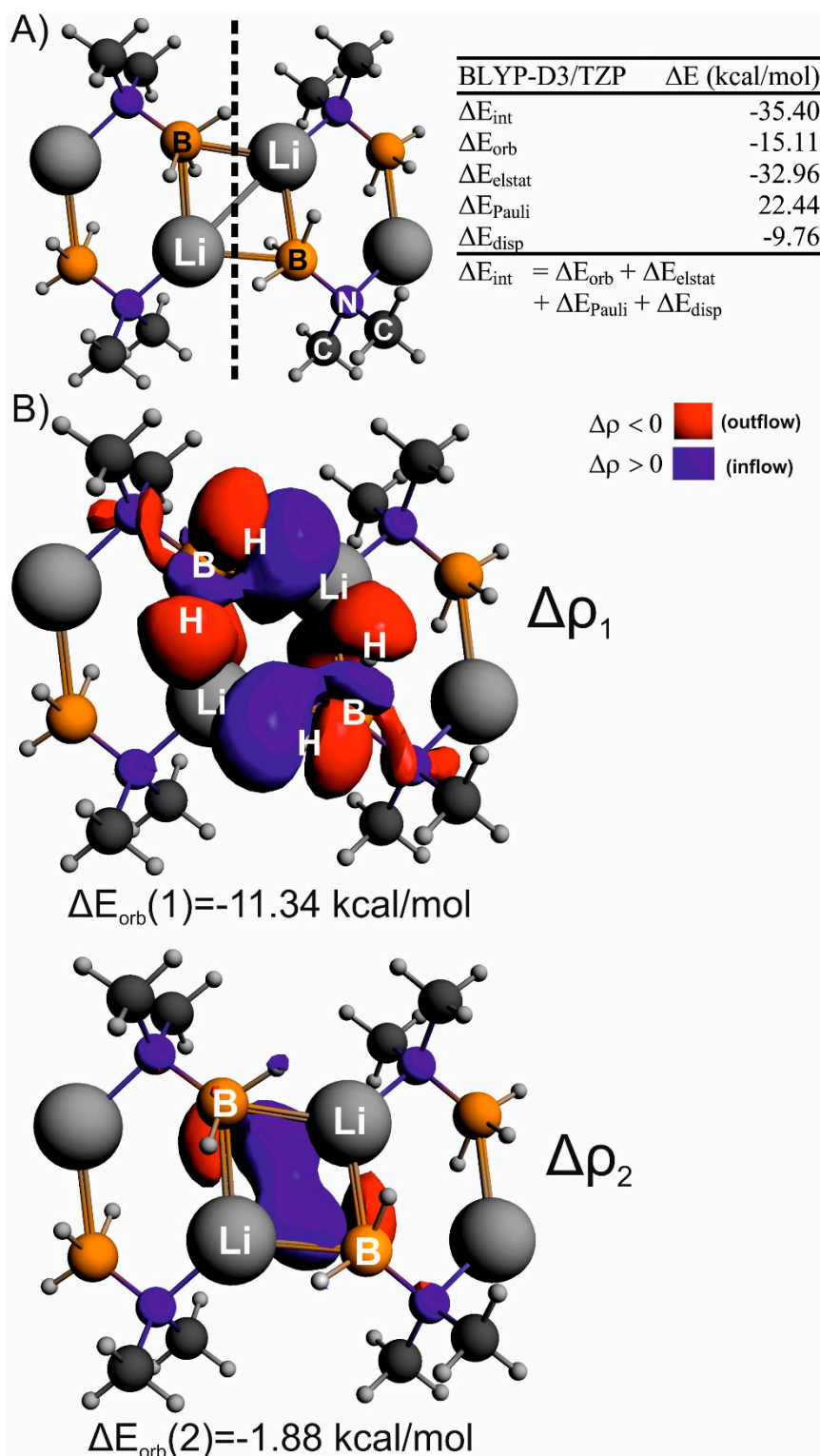


Figure S2. The tetrameric cluster model of $\text{LiN}(\text{CH}_3)_2\text{BH}_3$ directly taken from the crystal structure along with energy decomposition results describing the interaction between two dimeric fragments in $\text{LiN}(\text{CH}_3)_2\text{BH}_3$ (part A). Fragmentation pattern used in ETS-NOCV analysis is indicated by black dotted line. Part (B) displays the most relevant deformation density contributions describing $\text{Li}\cdots\text{H}-\text{B}$ interactions. Red color of deformation densities shows charge depletion, whereas blue an electron accumulation due to $\text{Li}\cdots\text{H}-\text{B}$ interaction.

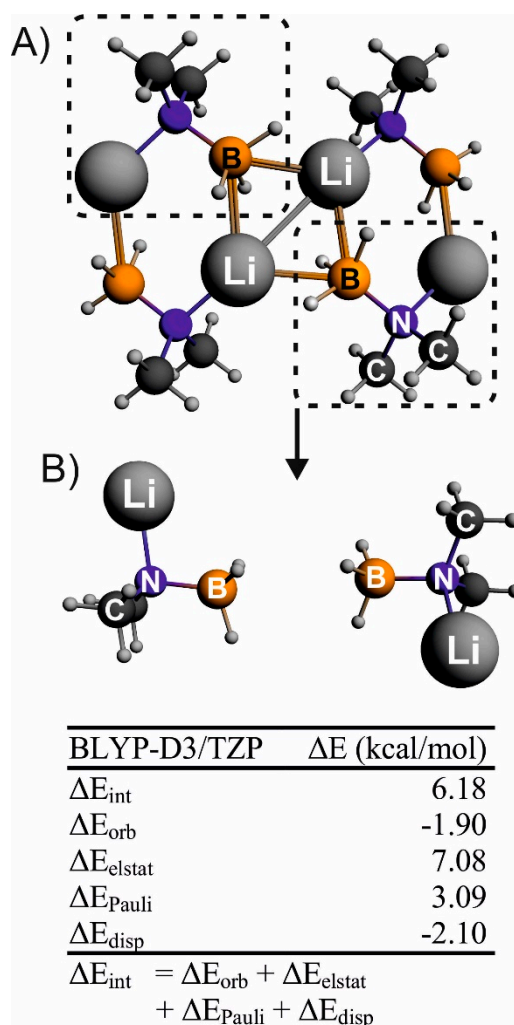


Figure S3. Dimer of $\text{LiN}(\text{CH}_3)_2\text{BH}_3$ from the crystal structure containing $\text{BH}\cdots\text{B}$ interactions together with results of ETS-NOCV analysis (in part (B)). Dimer was cut from the crystal structure as it is marked with black dotted lines (part (A)).

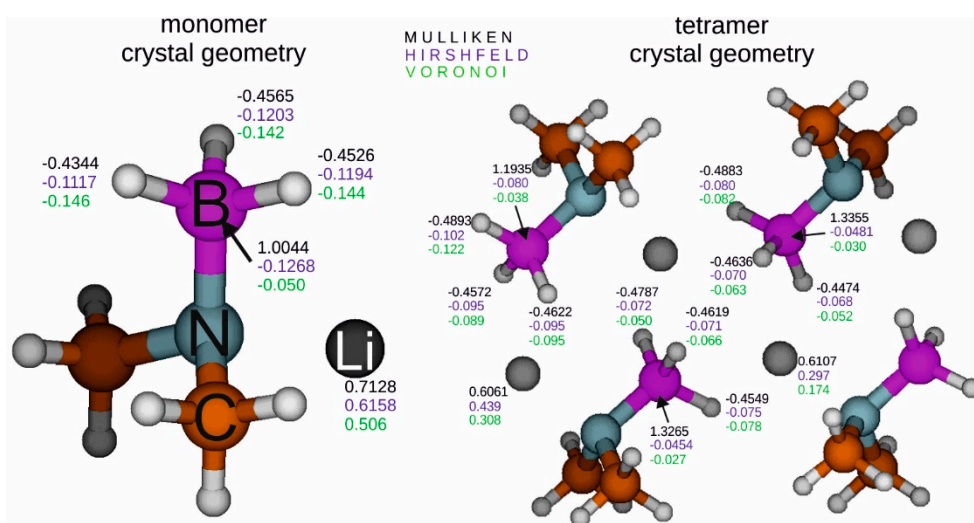


Figure S4. Atomic charges for the monomer and crystal tetramer of $\text{LiNMe}_2\text{BH}_3$ obtained from the Mulliken (black), Voronoi (green) and Hirshfeld (blue) approaches.

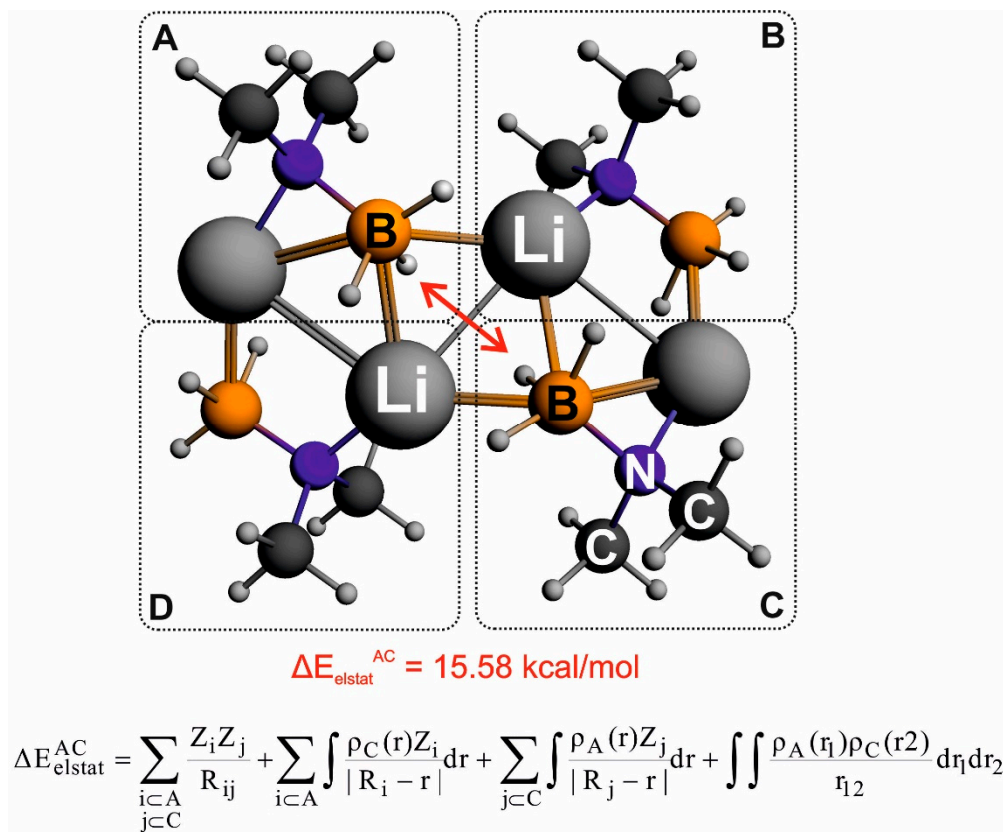


Figure S5. The electrostatic interaction between the monomers of $\text{LiNMe}_2\text{BH}_3$ connected through BH_3 units (A,C) calculated in the presence of the remaining two monomers (B,D).

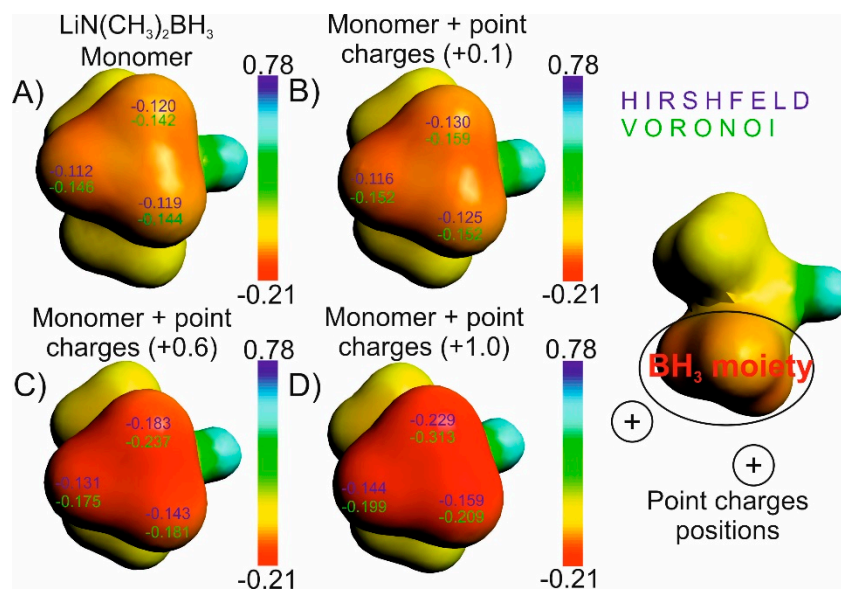


Figure S6. The contours of molecular electrostatic potential for the $\text{LiNMe}_2\text{BH}_3$ monomer in the presence of point charges (placed in the Li positions) with different values: +0.1 a.u., +0.6 a.u. and 1.0 a.u. In addition Hirshfeld and Voronoi atomic charges are depicted.